

# **Summertime Precipitation Variability over Europe and its Links to Atmospheric Dynamics and Evaporation**

**Igor I. Zveryaev and Richard P. Allan\***

P.P. Shirshov Institute of Oceanology, RAS, Moscow, Russia

\*Environmental Systems Science Centre, University of Reading, Reading, UK

*Submitted to JGR-Atmospheres*

*September, 2008*

Address for correspondence:

Dr. Igor I. Zveryaev, P.P. Shirshov Institute of Oceanology, RAS

36, Nakhimovsky Ave., Moscow, 117997, Russia

Telephone: 7 (495) 1247928

Telefax: 7 (495) 1245983

Email: [igorz@sail.msk.ru](mailto:igorz@sail.msk.ru)

## **Abstract**

A gridded monthly precipitation data for 1979-2006 from the Global Precipitation Climatology Project (GPCP) dataset are used to investigate interannual summer precipitation variability over Europe and its links to regional atmospheric circulation and evaporation.

The first EOF mode of European precipitation, explaining 17.2-22.8% of its total variance, is stable during summer season and is associated with the North Atlantic Oscillation (NAO). The spatial-temporal structure of the second EOF mode is less stable and shows essential month-to-month variations during summer season. This mode demonstrates rather strong link to the Scandinavian teleconnection pattern.

Analysis of links between leading EOF modes of regional precipitation and evaporation has revealed strong link between precipitation and evaporation from the European land surface, thus indicating an important role of the local processes in summertime precipitation variability over Europe. Weaker, but statistically significant links have been found for evaporation from the surface of the Mediterranean and Baltic Seas. Finally, in contrast to winter no significant links have been revealed between European precipitation and evaporation in the North Atlantic during summer season.

## 1. Introduction

Variability of regional precipitation on the short- and long-term time scales significantly impacts living conditions and different kinds of human activities in European region. Climate anomalies resulting in deficient/excessive precipitation may cause serious (and even catastrophic) socio-economic consequences. Recently, there were several examples of such climate anomalies in different parts of Europe that resulted in significant damage to the regional economies [e.g., *Christensen and Christensen, 2003; Schär et al., 2004; Marsh and Hannaford, 2007*]. Many recent regional climate extremes occurred during summer. However, compared to winter, significantly less attention has been given to analysis of European climate variability during summer season [e.g., *Colman and Davey, 1999; Hurrell and Folland, 2002; Zveryaev, 2004*]. In general, summertime climate variability in European region is not well studied and not well understood. Moreover, predictability of the climate in mid-latitudes for the summer season shows generally lower skills than that for the winter season [e.g., *Johansson et al., 1998; Colman and Davey, 1999; Dirmeyer et al., 2003; Koenigk and Mikolajewicz, 2008*]. In particular, basing on analysis of the North Atlantic sea surface temperature anomalies, *Colman and Davey [1999]* found quite low skills of statistical predictability of European climate during summer. Therefore, to improve prediction of regional climate and its extremes, particularly for the warm season, further analysis of the processes driving European climate variability is necessary.

In contrast to winter, when European precipitation variability is mostly driven by the North Atlantic Oscillation [NAO, e.g., *Hurrell, 1995; Qian et al., 2000; Zveryaev, 2006*], mechanisms driving interannual variability of regional precipitation during summer are more complex and are not well understood. In summer, when the role of atmospheric circulation in precipitation variability is diminished, the role of the local land surface processes increases [*Trenberth, 1999*].

Some studies point to importance of the land surface processes in summer precipitation variability [*Koster and Suarez, 1995; Schär et al., 1999; Seneviratne et al., 2006*], whereas other works highlight the role of the summer atmospheric circulation [*Pal et al., 2004; Koster et al., 2004; Ogi et al., 2005*]. Although the above mechanisms are not mutually exclusive, there is a high degree of uncertainty regarding their role in summer precipitation variability in Northern Hemisphere extra-tropics, and particularly over Europe.

Present study focuses on the analysis of the summer precipitation variability over Europe on interannual time scale, and on the links between this variability and regimes of the atmospheric circulation in the Atlantic-European sector. Furthermore, we investigate links between European precipitation and evaporation from the surface of the North Atlantic Ocean, Mediterranean and Baltic Seas, and from the European land surface. We analyze variability of precipitation over Europe on the basis of data available from the Global Precipitation Climatology Project (GPCP) dataset for 1979-2006 [*Huffman et al., 1997; Adler et al., 2003*]. In order to get more detailed information on the summer precipitation variability and to examine stability of the leading modes of precipitation during summer season, we performed analysis for summer seasonal mean precipitation as well as separate analyses for each summer month. The paper is organized as follows. The data used and analysis methods are described in section 2. Spatial-temporal structure of the leading modes of the summer seasonal and monthly mean precipitation variability for 1979-2006 is analyzed in section 3. Links between leading modes of precipitation variability and atmospheric circulation and teleconnection patterns are examined in section 4. In section 5 we explore links between regional precipitation and evaporation during summer season. Finally, concluding remarks are presented in section 6.

## 2. Data and methods

We employed monthly mean global precipitation data ( $2.5^\circ \times 2.5^\circ$  latitude-longitude grid) from the Version-2 of the GPCP dataset for 1979-2006 [Huffman *et al.*, 1997; Adler *et al.*, 2003]. The GPCP data set represents a combination of gauge observations and satellite estimates. Input data sets for the GPCP product include Global Precipitation Climatology Centre (GPCC) rain gauge analyses, SSM/I rain-rate estimates, GPI, rain gauge data from the Global Historical Climate Network (GHCN) and Climate Assessment and Monitoring System (CAMS), TOVS-based estimates and OLR precipitation index (OPI). The GPCP data are available online at <http://www.ncdc.noaa.gov/oa/wmo/wdcamet-ncdc.html>. In the present study the domain of analysis is limited to latitudes  $31.25^\circ\text{N}$ - $73.75^\circ\text{N}$  and longitudes  $13.75^\circ\text{W}$ - $51.25^\circ\text{E}$ .

In this study we also used evaporation data from the Woods Hole Oceanographic Institution (WHOI) data set [Yu and Weller, 2007]. In contrast to other flux products constructed from one single data source, this data set is determined by objectively blending the data sources from satellite and NWP model outputs while using in situ observations to assign the weights [Yu *et al.*, 2004; Yu and Weller, 2007]. The WHOI data set provides evaporation data ( $2.5^\circ \times 2.5^\circ$  latitude-longitude grid) over global oceans for 1958-2006. Detailed description of the data and the synthesis procedure can be found in Yu and Weller [2007] and at the website <http://oaflex.whoi.edu>. Since observational data over land are rather scarce, as a complementary data source on evaporation over land surface we used data from the NCEP/NCAR Reanalysis for 1979-2006 [Kalnay *et al.*, 1996]. These data are purely model-generated product. Thus, not pretending to get accurate quantitative estimates of the links between land surface evaporation and regional precipitation, we nevertheless, hope to obtain reasonable qualitative assessments of these links within degree of uncertainty provided by the reanalysis product.

To assess the links between variability of European precipitation and regional atmospheric circulation we use indices of the major teleconnection patterns that have been documented and described by *Barnston and Livezey* [1987]. The patterns and indices were obtained by applying rotated principal component analysis to standardized 500hPa height anomalies over Northern Hemisphere. In our analysis along with links to the NAO we examine links to such teleconnections as East Atlantic (EA) pattern, East Atlantic – West Russia (EAWR) pattern, and Scandinavian (SCA) pattern, which can also affect European precipitation variability. Regularly updated indices of these patterns are available from the Climate Prediction Center (CPC) website <http://www.cpc.ncep.noaa.gov/data/teledoc/telecontents.html>. The data cover the period 1950 - present. Details on the teleconnection pattern calculation procedures can be found in *Barnston and Livezey* [1987] and at the CPC website. To reveal dynamical context of the leading modes in precipitation variability, we used monthly sea level pressure data from the NCEP/NCAR Reanalysis for 1979-2006 [*Kalnay et al.*, 1996], having a 2.5° latitude by 2.5° longitude spatial resolution.

We examine a spatial-temporal structure of the long-term variations of summer monthly and seasonal mean precipitation over Europe by application of empirical orthogonal functions (EOF) analysis based on the covariance matrix [*Wilks*, 1995; *von Storch and Navarra*, 1995]. Prior to the EOF analysis the annual cycle was removed from all grid point time series by subtracting from each seasonal (monthly) value the respective season's (month's) long-term mean. After that the time series has been linearly detrended. In order to take into account the latitudinal distortions, obtained anomalies were weighted by the square root of cosine of latitude to ensure that equal areas are afforded equal weight in the analysis [*North et al.*, 1982].

To assess links to teleconnection patterns we use conventional correlation analysis. No lead or lag relationships were taken into consideration for this work; our analysis was restricted to simultaneous connections between precipitation variability over Europe and major teleconnection patterns and SLP fields in the North Atlantic - European sector. According to the Student's *t*-test [Bendat and Piersol, 1966], the minimum significant correlation coefficients between the time series analyzed are 0.374 for the 95% significance level. It is worth noting that the significance level of the correlation coefficient might be reduced if the time series are influenced by autocorrelation. More specifically, large lag-one autocorrelations reduce significantly effective number of degrees of freedom, while influence of small autocorrelations is weak [e.g., Bretherton *et al.*, 1990]. We examined the potential impact of autocorrelation on the estimation of significance of correlation coefficients, and our analysis did not reveal significant autocorrelations in considered time series (i.e., principal components of the leading EOF modes and teleconnection indices).

### **3. Leading modes of the summer precipitation variability over Europe**

To reveal the leading modes of interannual variability of precipitation over Europe during summer, we performed the EOF analysis on time series of the summer (June-July-August) mean and (separately) June, July and August monthly mean precipitation from the GPCP data set for the period 1979 – 2006. The motivation for the separate analyses of the monthly precipitation time series is based on our intention to examine stability of the leading EOF modes during summer season. We limit our analysis to consideration of the first and second EOF modes, because each of the subsequent modes explains less than 10% of the total precipitation variance, and because significant links between those modes of precipitation variability and regimes of

atmospheric circulation have not been revealed. It should be noted that in August the leading EOF modes of precipitation are not well separated according to the North criteria [North *et al.*, 1982], however, we include them into our consideration for the sake of completeness of analysis. Spatial patterns of the first two EOF modes of precipitation and time series of the corresponding principal components (hereafter PC) are shown, respectively, in Figures 1 and 2.

The first EOF mode explains from 17.2% (in June) to 22.8% (in July) of the total variance of precipitation. The respective spatial patterns (Figure 1a,c,e,g), characterized by a tripole-like structure, depict three action centers. The major action center extends from the British Isles to wide region around the Baltic Sea, and further to eastern Europe and European Russia. Two other centers of opposite polarity are located to south (i.e. over Mediterranean region) and north (i.e. over northern Scandinavia) off the major action center (Figure 1a,c,e,g). Structurally the obtained patterns are very similar to that of the first EOF mode of the mean summer precipitation from the CMAP data for 1979-2001 [Zveryaev, 2004]. We note that the structure of the EOF-1 patterns demonstrates evident persistence during summer season. In other words, structural changes from month to month are not significant, albeit local (i.e. in action centers) changes in magnitudes of variability are noticeable. The PC-1 (Figure 2a,c,e,g), displaying temporal behavior of this mode, demonstrates evident correspondence with the NAO index in all considered months and in analysis of seasonal mean precipitation. Moreover, high correlations between respective PCs and the NAO index (Table1) clearly indicate that during entire summer season EOF-1 of European precipitation is associated with the NAO. It should be noted, however, that summer NAO is essentially different (in terms of its spatial structure) from its winter counterpart [Barnston and Livezey, 1987]. Hence, the NAO-associated summer

precipitation patterns (Figure 1a,c,e,g) are also principally different from the winter dipole-like patterns [e.g., *Hurrell, 1995; Zveryaev, 2004*].

The second EOF mode of summer precipitation over Europe accounts for 12.4-15.3% of its total variance. The spatial pattern of this mode (Figure 1b,d,f,h) in general represents a meridional dipole characterized by the coherent precipitation variations over northern part of European Russia and Scandinavia and opposite variations over the remaining part of Europe. In particular, such pattern is well depicted in July (Figure 1f). However, in contrast to the first EOF, there are evident month-to-month changes in the structure of the second EOF mode. For example, in June (Figure 1d) the largest loadings are observed over western Europe and western Scandinavia, whereas in July (Figure 1f) they are revealed over eastern Europe and European Russia. In August (Figure 1h) the entire dipole demonstrates zonal rather than meridional orientation. Therefore, the second EOF mode of precipitation is less stable during summer season compared to the first mode. Figures 2d,f,h and results of correlation analysis (Table 1) imply that this mode of European precipitation is driven mainly by the SCA teleconnection pattern [*Barnston and Livezey, 1987*], consisting of the major action center over Scandinavia, and minor action centers of opposite polarity over western Europe and eastern Russia. Note, however, the second EOF mode of summer mean precipitation does not demonstrate significant link to the mean summer SCA index. We presume that possible reason for that is that the mean summer SCA index is defined not as respective EOF mode obtained from analysis of summer mean 500hPa geopotential heights (CPC does not provide such seasonal indices), but as the average from the SCA indices estimated for June, July and August. Since interannual behavior of these monthly indices is rather different (Figures 2d,f,h), their average hardly can be viewed as a

representative parameter reflecting interannual variability of summer mean atmospheric circulation.

Summarizing results of this section, we note that during summer the first EOF mode of European precipitation is stable (in terms of its month-to-month variations) and is strongly linked to the major regional climate signal – the NAO. The second EOF mode of regional precipitation is less stable and demonstrates some structural changes during summer season. Our results suggest that the major driver for this mode is the SCA teleconnection pattern [Barnston and Livezey, 1987]. To get deeper insight into regional atmospheric circulation that drives summer precipitation variability over Europe in the next section we analyze variability of the sea level pressure (SLP) and 500hPa fields in Atlantic-European sector and its links to European precipitation. Since there is general consistency between leading EOF modes of precipitation estimated for different summer months, and in order to avoid repetition, we limit our further analysis to consideration of the links between leading modes of July (presumably most representative summer month) precipitation and variability of other climate parameters estimated for this month.

#### **4. Links to regional atmospheric circulation**

To explore links between European precipitation and the leading modes of atmospheric circulation in July we first reveal these modes by applying EOF analysis to detrended and weighted SLP and 500hPa time series from the NCEP/NCAR reanalysis for 1979-2006. The domain of EOF analysis is the North Atlantic - European sector limited to latitudes 20°N-80°N and longitudes 70°W-70°E. Spatial patterns of the first and second EOF modes of SLP and 500hPa are shown in Figure 3.

The first EOF mode of July 500hPa heights and SLP in Atlantic-European sector contributes respectively 24.0% and 26.4% to their total variance. The spatial pattern of this mode (Figures 3a,c) represents the summer NAO, and shows a good agreement with July NAO pattern presented by *Barnston and Livezey* [1987]. The major difference of presented patterns from the typical winter NAO pattern [*e.g.*, *Hurrell*, 1995] is significant northeastward shift of the southern action center associated with Azores high during winter. As seen, in July this action center covers large part of Europe (Figures 3a,c), and along with respective pattern of July precipitation (Figure 1e), suggests that anti-cyclonic (cyclonic) anomaly results in deficient (excessive) precipitation over large portion of Europe. In general, presented patterns of the first EOF mode of 500hPa heights and SLP illustrate significant seasonal (i.e. from winter to summer season) northward shift of the North Atlantic storm track. As expected, PCs of this mode (not shown) are strongly correlated to the July NAO index and to PCs of the first EOF mode of July precipitation (Table 2).

The second EOF mode explains 16.1% of total July 500hPa variance, and 16.8% of July SLP variance. The spatial patterns (Figures 3b,d) of this mode are characterized by two dominating action centers located over northeastern North Atlantic and over European Russia. Minor action centers of opposite polarity over Scandinavia, Greenland and western North Atlantic are seen in EOF-2 pattern for SLP (Figure 3d). Structurally the obtained EOF-2 patterns are similar to the EAWR pattern obtained by *Barnston and Livezey* [1987] and referred to as the Eurasia-2 pattern in their study. Further analysis of correlations between respective principal components and July EAWR index (Table 2) confirmed that the second EOF mode obtained from analysis of 500hPa and SLP fields in the North Atlantic – European sector does indeed represent the EAWR teleconnection pattern. It is important to emphasize that PCs of the EOF-2

of 500hPa and SLP are not correlated to the respective PCs of precipitation over Europe (Table 2). We remind that our analysis has shown (see previous chapter) that the second EOF mode of regional precipitation is associated with the Scandinavian teleconnection, previously referred to as the Eurasia-1 pattern in *Barnston and Livezey* [1987] study.

## **5. Links between European precipitation and regional evaporation**

In this chapter we examine links between European precipitation and evaporation in four regions that presumably can impact variability of European precipitation during warm season. These regions are the North Atlantic Ocean, the Baltic and Mediterranean Seas, and Europe (i.e., European land surface). We first reveal the leading modes of evaporation in each region by applying EOF analysis to detrended and weighted evaporation time series from the WHOI dataset (for oceanic/marine regions) and from the NCEP/NCAR reanalysis (for European land surface) for 1979-2006. Spatial patterns of the first and second EOF modes of evaporation for the Baltic Sea, Mediterranean Sea and Europe are shown respectively in Figure 4, Figure 5 and Figure 6. Further, we analyze links between leading EOF modes of evaporation in aforementioned regions and leading modes of precipitation over Europe. Since we did not find statistically significant links between European precipitation and evaporation in the North Atlantic during summer, we exclude this region from our further analysis. As we mentioned in previous chapter, the structure of the EOF-1 of SLP (Figure 3c) indicates significant northward shift (compared to winter) of the North Atlantic storm track. This suggests that the moisture evaporated in the North Atlantic is mostly transported to the Arctic basin rather than to Europe (as it usually happens during winter). Therefore, the fact that we did not find significant links between summertime European precipitation and evaporation in the North Atlantic is not so

surprising. Note, however, that local precipitation variability in some European regions (e.g., northern Scandinavia) can be influenced by the North Atlantic moisture transport.

We slightly extended domain of analysis for the Baltic Sea region since both the North Sea and Baltic Sea are influenced by the same atmospheric circulation patterns (Figure 3), and because amount of grid points covering the Baltic Sea is low. Due to latter reason we also re-gridded the WHOI data onto  $1^\circ \times 1^\circ$  grid. Along with EOF analysis of original data we performed analysis of re-gridded data (that was also done for the Mediterranean Sea). Both analyses gave very similar results. In Figures 4 and 5, we show smoother and “nicer” looking patterns based on analyses of re-gridded data.

In July the first EOF mode of evaporation in the extended Baltic Sea – North Sea region explains about half of its total variability. Its spatial pattern reflects coherent variations of evaporation over entire domain of analysis (Figure 4a). However principal components (not shown) of this mode do not demonstrate significant correlations to PC-1 and PC2 of precipitation, suggesting that this mode does not influence large-scale variability of European precipitation during summer. The second EOF mode of evaporation in the Baltic Sea – North Sea region accounts for 18.7% of its total variability in July. Its spatial pattern depicts a dipole with opposite variations of evaporation in the Baltic Sea and the North Sea (Figure 4b). Such pattern presumably reflects more local (compared to the first EOF mode) forcings of the regional evaporation variability. Principal components of this mode (not shown) demonstrate significant correlation to the EOF-1 of European precipitation (Table 3), suggesting influence of this mode on variability of regional precipitation. However, since the EOF-2 explains relatively low fraction of the total evaporation, we presume that this influence is not very large.

The first EOF mode of evaporation from the surface of the Mediterranean Sea in July explains 45.6% of its total variability. The spatial pattern of this mode is characterized by coherent variations of evaporation over entire Mediterranean Sea (Figure 5a). Principal components (not shown) of this mode correlate significantly to PC-1 of precipitation over Europe (Table 3), suggesting essential influence of this mode on summertime variability of regional precipitation. More specifically, Figures 1e and 5a indicate that below (above) normal precipitation over large part of Europe is associated with decreased (increased) evaporation from the surface of the Mediterranean Sea. The EOF-2 accounts for 21.3% of total variability of evaporation in the Mediterranean Sea region in July. Its spatial pattern is characterized by the zonal dipole with opposite variations of evaporation in the western and eastern parts of the sea (Figure 5b). Principal components of the EOF-2 (not shown) demonstrate significant correlation to the EOF-1 of European precipitation (Table 3) which is almost equal to that obtained for the PC-1. Thus, our results suggest that both the first and the second EOF modes, explaining together about 67% of total variability of Mediterranean evaporation, affect summertime variability of precipitation over Europe. Although aforementioned correlations are almost equal, the influence of the first EOF mode is indeed significantly larger since it explains twice larger fraction of the total variability of evaporation.

The spatial pattern of the EOF-1 of evaporation from the European land surface is characterized by the major action center covering almost entire Europe from Iberian Peninsula and France to Scandinavia and European Russia where the largest loadings are revealed (Figure 6a). Minor action center of opposite polarity is revealed over the Balkans and eastern Mediterranean – Black Sea region. This mode explains 24.9% of the total variability of regional evaporation. Principal components of this mode show high (0.78) correlation to the PC-1 of

European precipitation, suggesting a strong coupling between European precipitation and evaporation during warm season. Note the above correlation is the largest among those considered in our analysis (Table 3). The second EOF mode of evaporation from the European land surface in July explains only 12.8% of its total variability. Its spatial pattern represents a meridional dipole with opposite variations of evaporation north/south off approximately 53°-55°N latitude (Figure 6b). In contrast to EOF-1, principal components of this mode do not show significant correlations to the leading EOF modes of regional precipitation (Table 3).

To summarize results of this section, we note that our analysis suggests that, in contrast to winter season, during summer the evaporation in the North Atlantic does not affect continental-scale interannual variability of precipitation over Europe. However, smaller scale variability of precipitation, particularly in some coastal regions, can be significantly affected by this factor. Our analysis indicates significant role of land surface evaporation in variability of European precipitation during warm season. This result supports recent findings based on model simulations [*Koster and Suarez, 1995; Schär et al., 1999; Seneviratne et al., 2006*]. Note, however, that in contrast to the North Atlantic, Baltic and Mediterranean Seas where observation-based data were used, for the land surface we used evaporation from reanalysis product having well known limitations. We also found statistically significant links between evaporation in the Baltic and Mediterranean Seas and interannual variability of precipitation over Europe. However, we believe that the major regions affecting (through evaporation) regional precipitation during warm season are Mediterranean Sea and European land area, while evaporation in the Baltic Sea plays a minor role. Overall, results of this chapter suggest that in contrast to winter season when the moisture advection from the North Atlantic into European

region plays a dominant role in regional precipitation variability, during boreal summer local processes make major contribution to interannual variability of European precipitation.

## 6. Concluding remarks

In the present study we analyzed the leading modes of interannual variability of summertime precipitation over Europe based on the data from the GPCP dataset for 1979-2006 [Huffman *et al.*, 1997; Adler *et al.*, 2003]. We also investigated relation of these modes to regional atmospheric circulation, and their links to evaporation in the North Atlantic Ocean, Baltic and Mediterranean Seas, as well as to evaporation from the European land surface.

It is shown that the first EOF mode of European precipitation is rather stable (in terms of its spatial-temporal structure) during summer season, and is characterized by tripole-like pattern with large coherent variations over wide region extending from British Isles to European Russia. Relatively weak precipitation variations of opposite sign are revealed north and south off the above region. This mode is associated with the NAO [*e.g.*, Hurrell, 1995]. The second EOF mode of summer precipitation (characterized by meridional dipole structure) is less stable, and is linked to the Scandinavian teleconnection [Barnston and Livezey, 1987].

Analysis of links between European precipitation and evaporation has shown that, in contrast to winter season, when regional precipitation variability mostly determined by the NAO-driven moisture advection from the North Atlantic, summertime continental scale variability of precipitation is not associated with evaporation in the North Atlantic. This is due to significant northeastward shift of the North Atlantic storm track associated with the summer NAO structure that is principally different from its winter counterpart. On the contrary, our results suggest strong impact of the local processes, in particular land surface evaporation, on variability of

regional precipitation during warm season, thus, supporting recent model-based results of other studies [*e.g.*, Schär *et al.*, 1999; Seneviratne *et al.*, 2006]. However, since we used in our study reanalysis data having well known limitations, further analysis of the role of land surface evaporation in interannual variability of European precipitation during warm season is needed. We also found significant links between summertime European precipitation and evaporation in the Mediterranean Sea which also (along with land surface) can be viewed as a local (rather than remote) source of moisture. It seems that the influence of the Baltic Sea evaporation on regional precipitation is not large (although statistically significant links are detected) and probably limited to the Baltic region.

The present study highlights mechanisms driving summertime interannual variability of precipitation over Europe. Since the summertime NAO is structurally different from that for other seasons, its impact on summer precipitation variability over Europe is also principally different. We found that during summer the leading modes of regional precipitation are not associated with evaporation in the North Atlantic, but strongly linked to local processes such as evaporation from the European land surface and from the surface of the Mediterranean Sea. However, since our assessment of the links to land surface evaporation is limited to reanalysis product, we hope that further diagnostic studies of the observational data as well as model experiments will allow obtaining more accurate estimates of these links, thus, providing extremely useful information for the seasonal climate prediction for the European region.

## **Acknowledgments**

This research was supported by the Royal Society grant (International Incoming Short Visits). Major part of the present study has been performed during IIZ work at the Environmental

Systems Science Centre, University of Reading as a visiting scientist. IIZ was also supported by the Russian Foundation for Basic Research Grant 05-05-64908.

## References

- Adler, R.F., and coauthors (2003), The Version-2 Global Precipitation Climatology Project (GPCP) monthly precipitation analysis (1979-present), *J. Hydromet.*, **4**, 1147-1167.
- Barnston, A.G., and R.E. Livezey (1987), Classification, seasonality and persistence of low-frequency atmospheric circulation patterns, *Mon. Weather Rev.*, **115**, 1083-1126.
- Bendat, J.S., and A.G. Piersol (1966), *Measurement and Analysis of Random Data*, 390 pp., John Wiley, Hoboken, N. J.
- Briffa, K.R., and T.J. Osborn, (2002), Blowing hot and cold, *Science*, **295**, 2227-2228.
- Cassou, C., and L. Terray (2001), Oceanic forcing of the wintertime low-frequency atmospheric variability in the North Atlantic European sector: a study with the APREGGE model, *J. Clim.*, **14**, 4266-4291.
- Christensen, J.H., and O.B. Christensen (2003), Severe summertime flooding in Europe, *Nature*, **421**, 805-806.
- Colman, A., and M. Davey (1999), Prediction of summer temperature, rainfall and pressure in Europe from preceding winter North Atlantic ocean temperature, *Int. J. Climatol.*, **19**, 513-536.

Drevillon, M., L. Terray, P. Rogel, and C. Cassou (2001), Mid latitude Atlantic SST influence on European climate variability in the NCEP reanalysis, *Clim. Dyn.*, 18, doi:10.1007/s003820100178.

Huffman, G.J., and coauthors (1997), The Global Precipitation Climatology Project (GPCP) combined precipitation dataset, *Bull. Amer. Meteorol. Soc.*, 78, 5-20.

Hurrell, J.W. (1995), Decadal trends in the North Atlantic oscillation: Regional temperature and precipitation, *Science*, 269, 676-679.

Hurrell, J.W., and C.K. Folland (2002), A change in the summer atmospheric circulation over the North Atlantic, *CLIVAR Exch.*, 7(3-4), 52-54.

Kalnay, E., Kanamitsu, M., Kistler, R., Collins, W., Deaven, D., Gandin, L., Iredell, M., Saha, S., White, G., Wollen, J., Zhu, Y., Chelliah, M., Ebisuzaki, W., Higgins, W., Janowiak, J., Mo, K. C., Ropelewski, C., Wang, J., Leetma, A., Reynolds, R., Jenne, R. and D. Joseph (1996), The NCEP/NCAR 40-year reanalysis Project. *Bull. Amer. Met. Soc.*, 77, No. 3, 437-471.

Kerr, R.A. (2000), A North Atlantic climate pacemaker for the centuries, *Science*, 288, 1984-1985.

Koenigk, T., and U. Mikolajewicz (2008), Seasonal to interannual climate predictability in mid and high northern latitudes in a global climate model, *Clim. Dyn.*, 28, doi:10.1007/s00382-008-0419-1.

Koster, R.D., and M.J. Suarez (1995), Relative contributions of land and ocean processes to precipitation variability, *J. Geophys. Res.*, 100, D7, 13775-13790.

Koster, R.D., and coauthors (2004), Regions of strong coupling between soil moisture and precipitation, *Science*, 305, 1138-1140.

Lenderink, G., A. van Ulden, B. van den Hurk, and E. van Meijgaard (2007), Summertime interannual temperature variability in an ensemble of regional model simulations: analysis of surface energy budget, *Clim. Change*, 81, 233-247.

Marsh, T. J. and J. Hannaford (2007), The summer 2007 floods in England and Wales - a hydrological appraisal. Centre for Ecology & Hydrology. 32pp.

North, G.R., T.L. Bell, and R.F. Calahan (1982), Sampling errors in the estimation of empirical orthogonal functions, *Mon. Wea. Rev.*, 110, 699-706.

Ogi, M., K. Yamazaki, and Y. Tachibana (2005), The summer northern annular mode and abnormal summer weather in 2003, *Geophys. Res. Lett.*, 32, L04706.

Pal, J.S., F. Giorgi, and X. Bi (2004), Consistency of recent European summer precipitation trends and extremes with future regional climate projections, *Geophys. Res. Lett.*, 31, L13202.

Pauling, A., J. Luterbacher, C. Casty, and H. Wanner (2006), Five hundred years of gridded high-resolution precipitation reconstructions over Europe and the connection to large-scale circulation, *Clim. Dyn.*, 26, doi:10.1007/s00382-005-0090-8.

Portis, D.H., J.E. Walsh, M. El Hamly, and P.J. Lamb (2001), Seasonality of the North Atlantic Oscillation, *J. Clim.*, 14, 2069-2078.

Qian, B., H. Xu, and J. Corte-Real (2000), Spatial-temporal structures of quasi-periodic oscillations in precipitation over Europe, *Int. J. Climatol.*, 20, 1583-1598.

Rodwell, M.J., and C.K. Folland (2002), Atlantic air-sea interaction and seasonal predictability, *Q. J. R. Meteorol. Soc.*, 128, 1413-1443.

Seneviratne, S.I., D. Lüthi, M. Litschi, and C. Schär (2006), Land-atmosphere coupling and climate change in Europe, *Nature*, 443, 205-209.

Schär, C., D. Lüthi, and U. Beyerle (1999), The soil-precipitation feedback: a process study with a regional climate model, *J. Climate*, 12, 722-741.

Schär, C., D. Lüthi, and U. Beyerle (2004), The role of increasing temperature variability in European summer heatwaves, *Nature*, 427, 332-336.

Sutton, R.T., and D.L.R. Hodson (2005), Atlantic ocean forcing of North American and European summer climate, *Science*, 309, 115-118.

Trenberth, K.E. (1999), Atmospheric moisture recycling: Role of advection and local evaporation, *J. Climate*, 12, 1368-1381.

Trenberth, K.E., A. Dai, R.M. Rasmussen, and D.B. Parsons (2003), The changing character of precipitation, *Bull. Am. Meteorol. Soc.*, 84, 1205-1217.

Vidale, P.L., D. Lüthi, R. Wegmann, and C. Schär (2007), European summer climate variability in a heterogeneous multi-model ensemble, *Clim. Change*, 81, 209-232.

von Storch, H., and A. Navarra (1995), *Analysis of Climate Variability*, 334 pp., Springer-Verlag, New-York.

Wibig, J. (1999), Precipitation in Europe in relation to circulation patterns at the 500 hPa level, *Int. J. Climatol.*, 19, 253-269.

Wilks, D.S. (1995), *Statistical Methods in the Atmospheric Sciences*, 467 pp., Academic, San Diego, Calif.

Yu, L., and R.A. Weller (2007), Objectively analyzed air-sea heat fluxes for the global ice-free oceans (1981-2005), *Bull. Amer. Meteorol. Soc.*, **88**, 527-539.

Yu, L., R.A. Weller, and B. Sun (2004), Improving latent and sensible heat flux estimates for the Atlantic Ocean (1988-99) by a synthesis approach, *J. Climate*, **17**, 373-393.

Zolina, O., C. Simmer, A. Kapala, and S. Gulev (2005), On the robustness of the estimates of centennial-scale variability in heavy precipitation from station data over Europe, *Geophys. Res. Lett.*, **32**, L14707, doi: 10.1029/2005GL023231.

Zveryaev, I.I. (2004), Seasonality in precipitation variability over Europe, *J. Geophys. Res.*, **109**, D05103, doi:10.1029/2003JD003668.

Zveryaev, I.I. 2006. Seasonally varying modes in long-term variability of European precipitation during the 20th century. *J. Geophys. Res.* **111**, D21116, doi: 10.1029/2005JD006821.

## **Table Captions**

**Table 1.** Correlation coefficients between PC-1 and PC-2 of summer, June, July and August precipitation, and indices of teleconnection patterns. Coefficients, shown in bold, are statistically significant at the 95% significance level.

**Table 2.** Correlation coefficients between PC-1 and PC-2 of July SLP, 500hPa fields, and precipitation, and indices of teleconnection patterns. Coefficients, shown in bold, are statistically significant at the 95% significance level.

**Table 3.** Correlation coefficients between PC-1 and PC-2 of July precipitation, and evaporation in different regions. Coefficients, shown in bold, are statistically significant at the 95% significance level.

## Figure Captions

**Figure 1.** Spatial patterns of the first two EOF modes of the summer mean (a, b), June (c, d), July (e, f) and August (g, h) GPCP precipitation (1979-2006). Red (blue) color indicates positive (negative) values.

**Figure 2.** Principal components of the first two EOF modes of the summer mean (a, b), June (c, d), July (e, f) and August (g, h) GPCP precipitation (1979-2006). Blue (green) curves depict the NAO (SCA) index.

**Figure 3.** Spatial patterns of the first two EOF modes of July 500hPa (a, b) and SLP (c, d) fields (1979-2006). Red (blue) color indicates positive (negative) values.

**Figure 4.** Spatial patterns of the first two EOF modes of July evaporation in the Baltic Sea – North Sea region (1979-2006). Red (blue) color indicates positive (negative) values.

**Figure 5.** Spatial patterns of the first two EOF modes of July evaporation from the surface of Mediterranean Sea (1979-2006). Red (blue) color indicates positive (negative) values.

**Figure 6.** Spatial patterns of the first two EOF modes of July evaporation from the European land surface (1979-2006). Red (blue) color indicates positive (negative) values.

**Table 1.** Correlation coefficients between PC-1 and PC-2 of summer, June, July and August precipitation, and indices of teleconnection patterns. Coefficients, shown in bold, are statistically significant at the 95% significance level.

	<b>Summer</b>		<b>June</b>		<b>July</b>		<b>August</b>	
	PC-1	PC-2	PC-1	PC-2	PC-1	PC-2	PC-1	PC-2
NAO	<b>0.67</b>	0.14	<b>0.68</b>	0.48	<b>0.50</b>	-0.12	<b>0.63</b>	0.04
SCA	0.10	0.30	-0.16	<b>0.76</b>	-0.21	<b>0.65</b>	-0.26	<b>0.49</b>

**Table 2.** Correlation coefficients between PC-1 and PC-2 of July SLP, 500hPa fields, and precipitation, and indices of teleconnection patterns. Coefficients, shown in bold, are statistically significant at the 95% significance level.

	<b>SLP</b>		<b>500hPa</b>	
	PC-1	PC-2	PC-1	PC-2
PRE PC-1	<b>0.85</b>	-0.31	<b>0.91</b>	0.23
PRE PC-2	0.15	0.17	-0.16	-0.09
NAO	<b>0.73</b>	0.04	<b>0.49</b>	-0.07
EAWR	0.13	<b>0.74</b>	0.24	<b>0.72</b>

**Table 3.** Correlation coefficients between PC-1 and PC-2 of July precipitation, and evaporation in different regions. Coefficients, shown in bold, are statistically significant at the 95% significance level.

<b>Europe Precip.</b>	<b>N. Atlantic</b>		<b>Baltic</b>		<b>Mediterranean</b>		<b>Europe</b>	
	EVA1	EVA2	EVA1	EVA2	EVA1	EVA2	EVA1	EVA2
PRE1	-0.14	***	0.04	<b>0.48</b>	<b>0.43</b>	<b>-0.42</b>	<b>0.78</b>	0.34
PRE2	0.10	***	-0.16	0.17	-0.21	0.23	-0.26	0.30

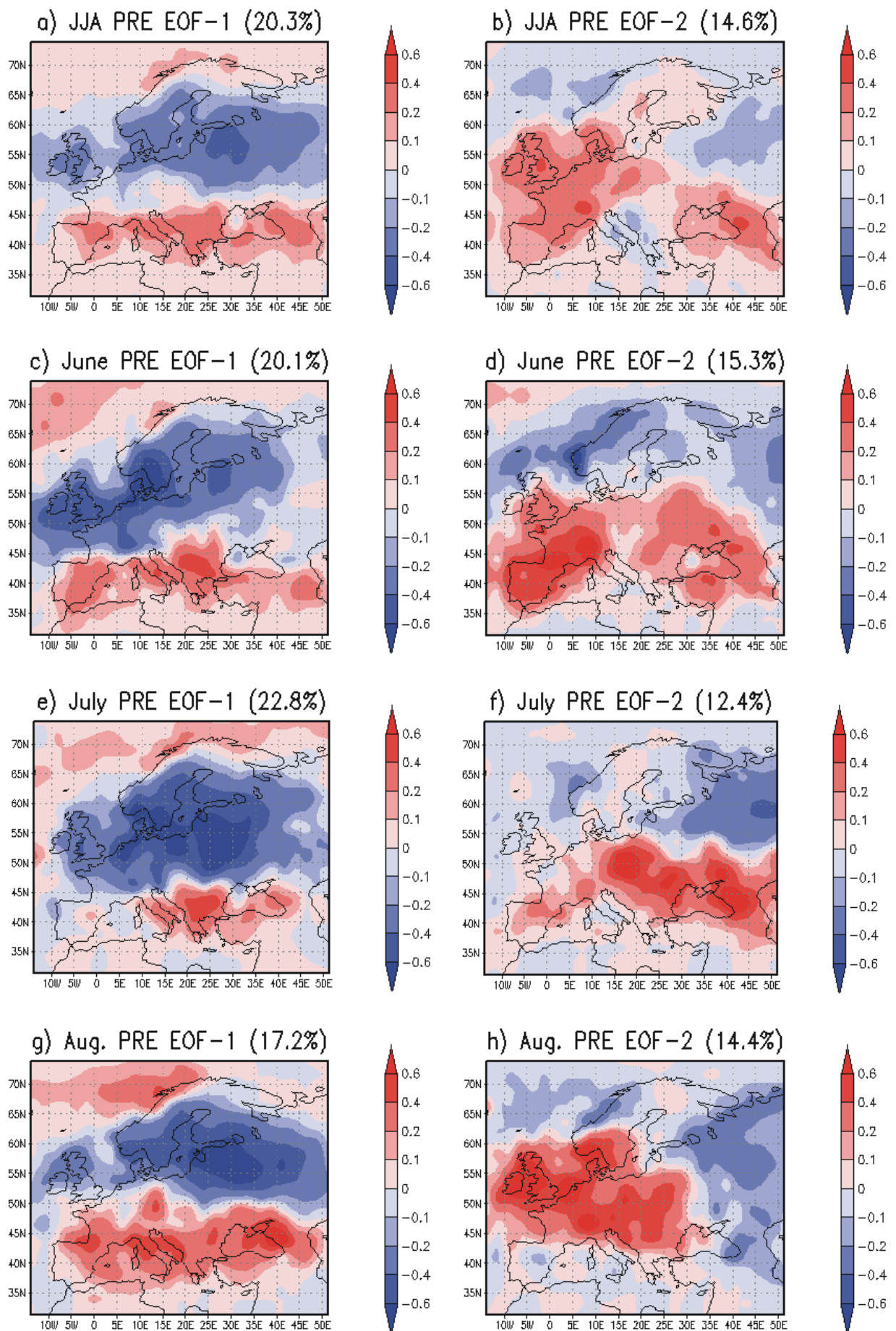


Figure 1.

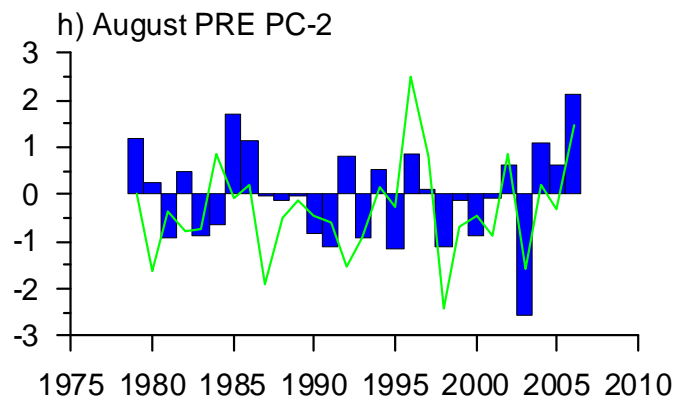
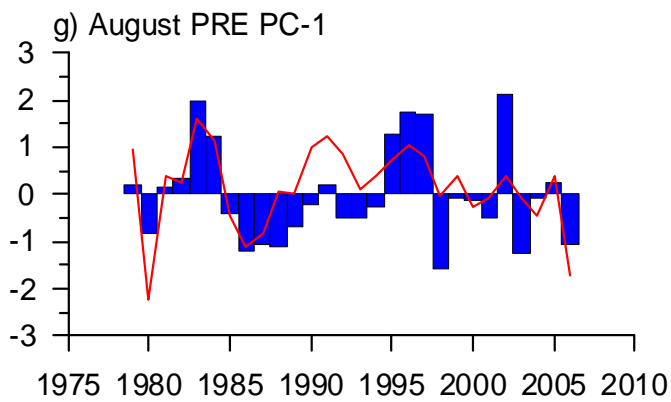
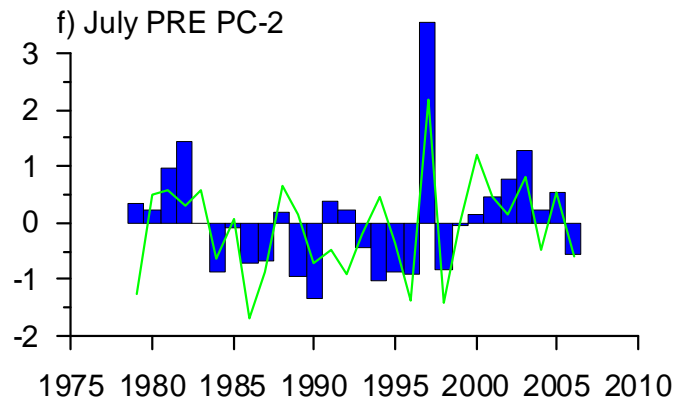
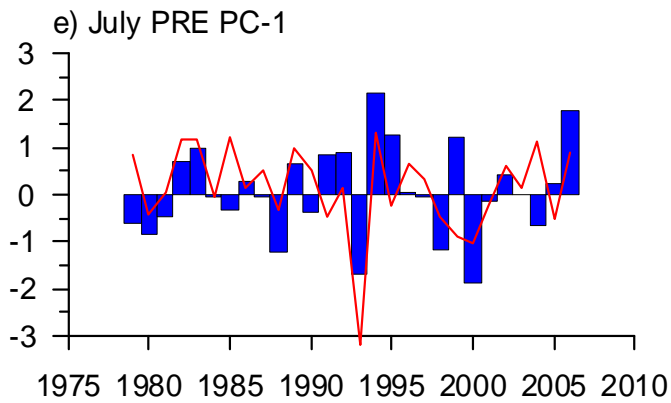
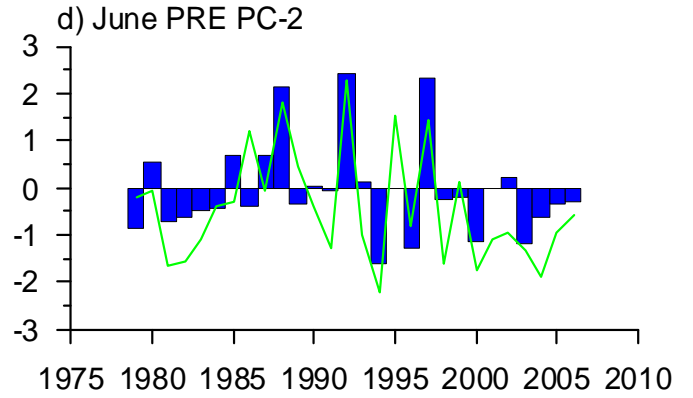
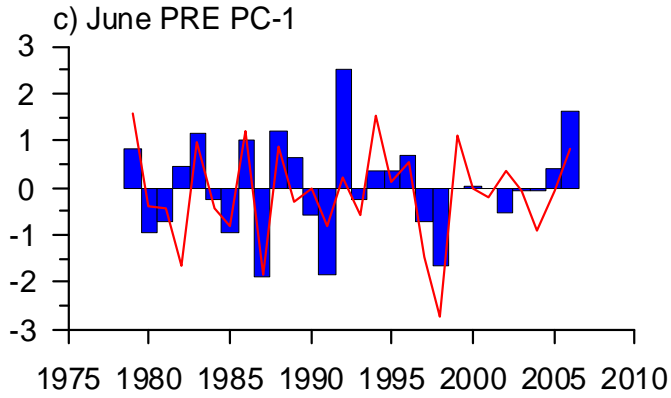
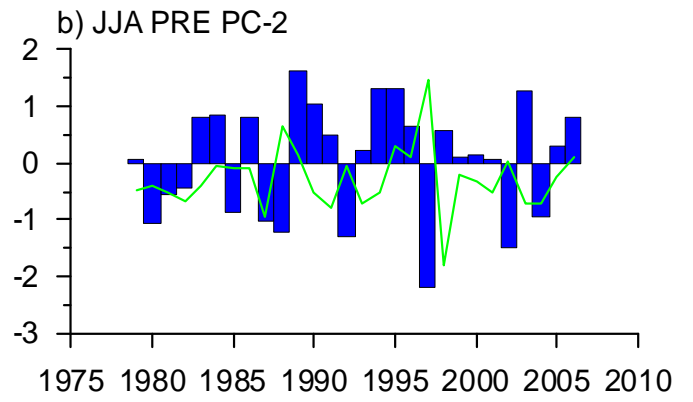
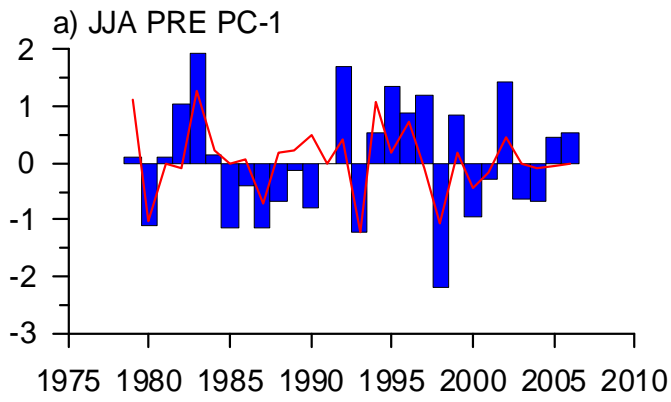


Figure 2.

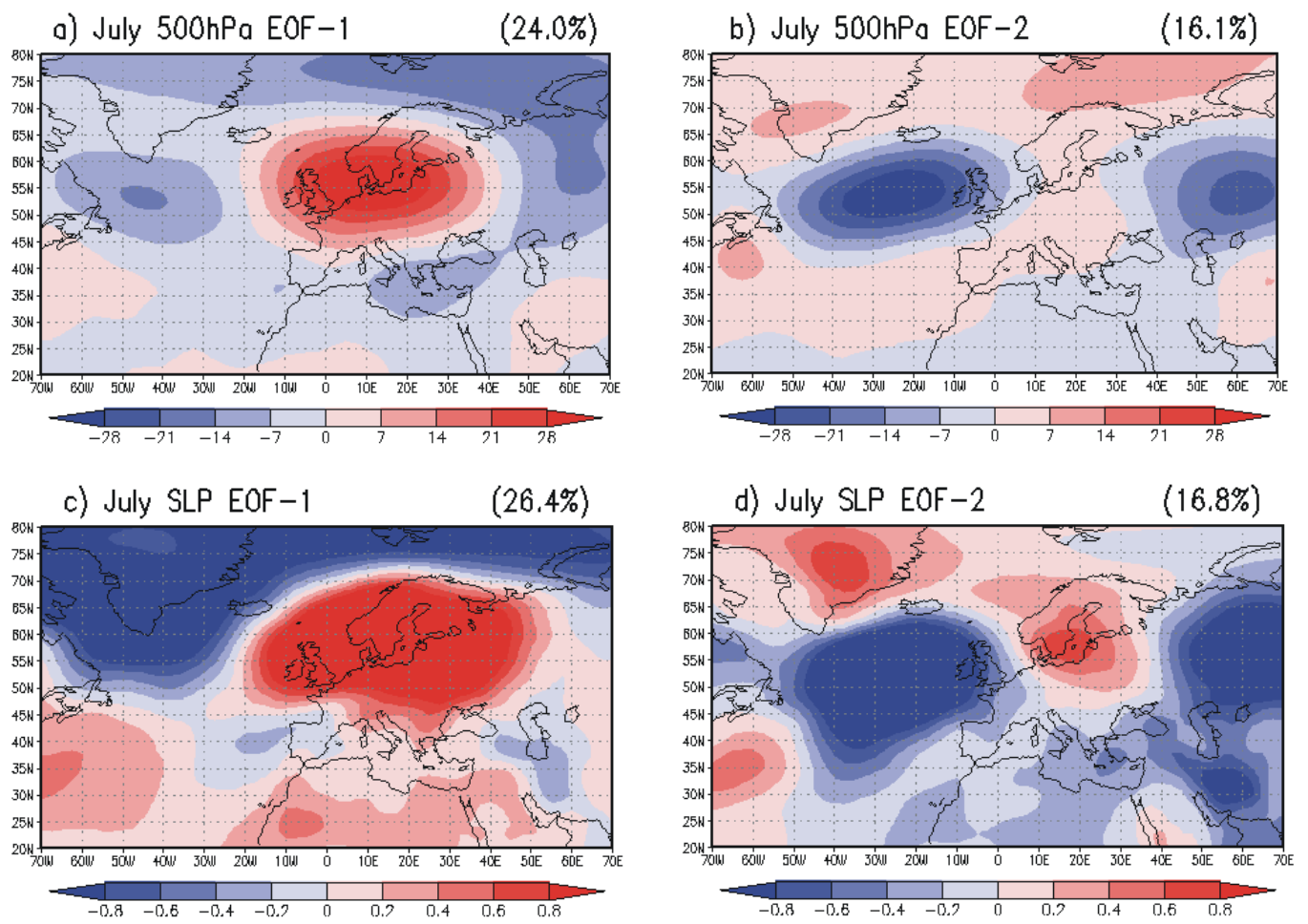


Figure 3.

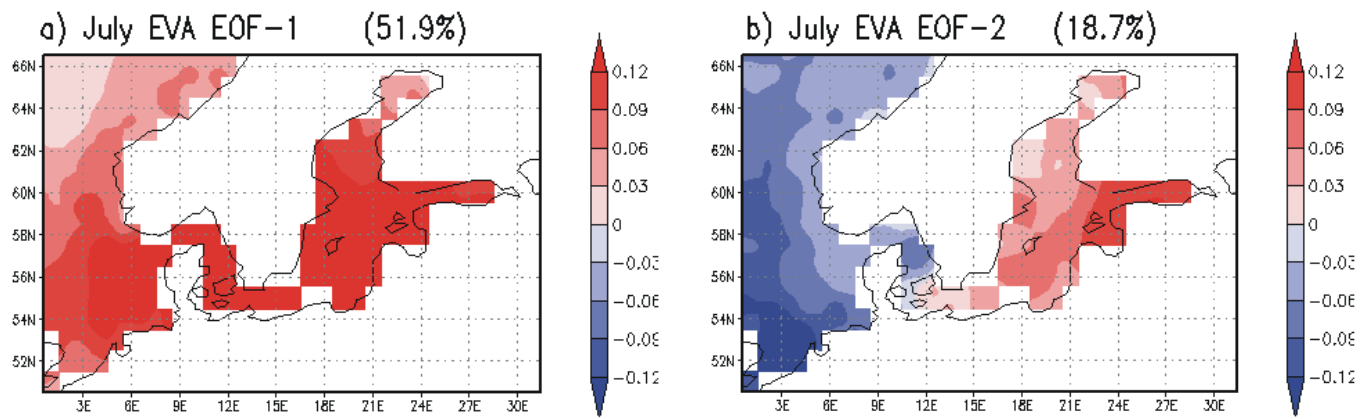


Figure 4.

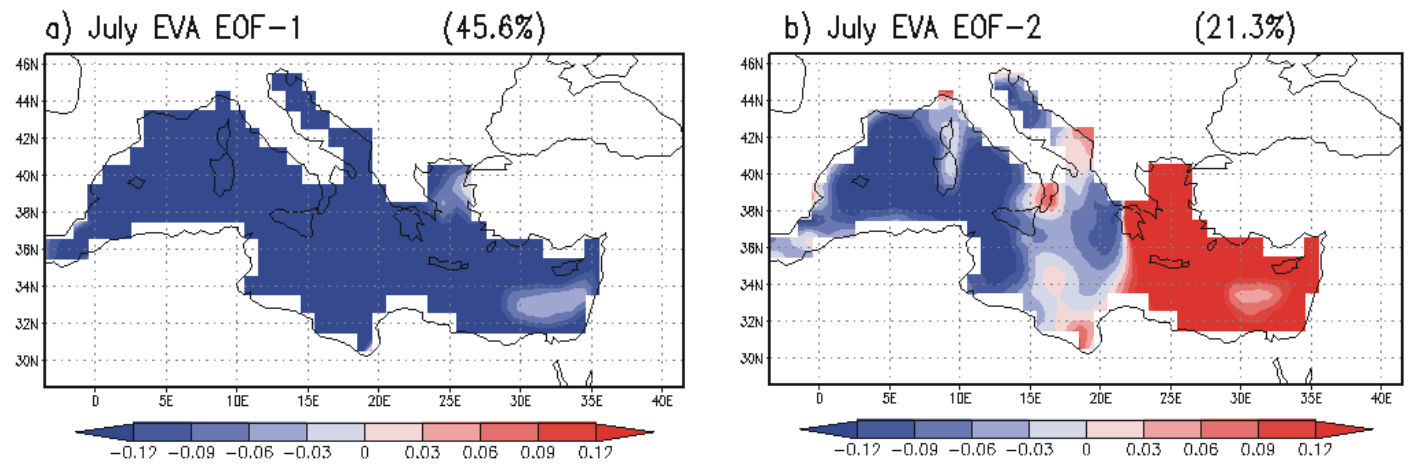


Figure 5.

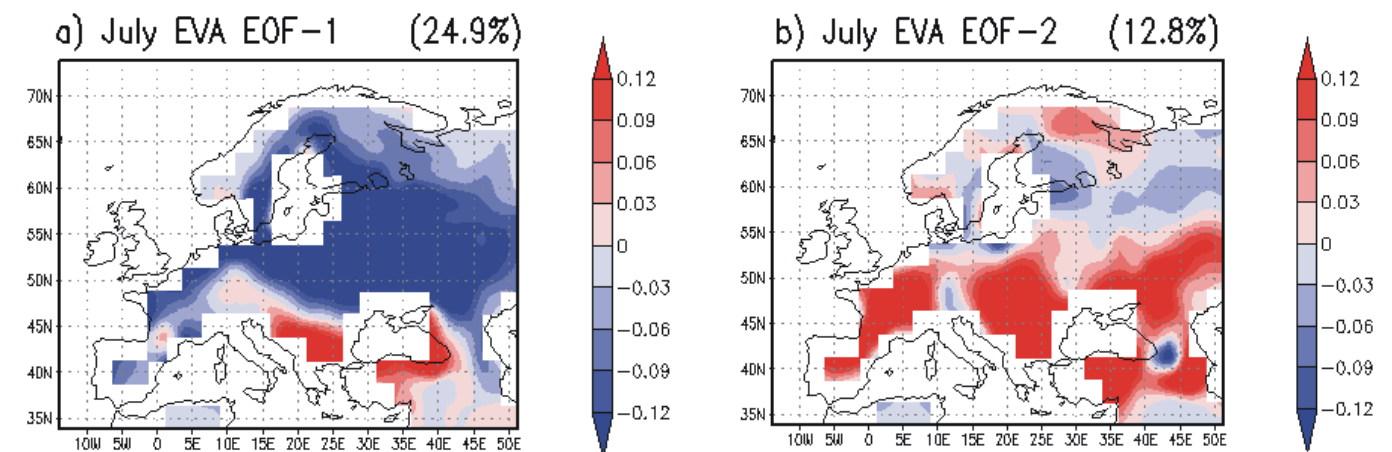


Figure 6.